GEOPHYSICAL RESEARCH LETTERS, VOL. 41, 102–107, doi:10.1002/2013GL058193, 2014

Quantifying upper ocean turbulence driven by surface waves

E. A. D'Asaro,[1,2] J. Thomson,[1,3] A. Y. Shcherbina,[1] R. R. Harcourt,[1] M. F. Cronin,[4] M. A. Hemer,[5] and B. Fox-Kemper[6]

Received 1 October 2013; revised 4 December 2013; accepted 6 December 2013; published 8 January 2014.

[1] Nearly all operational ocean models use air-sea fluxes and the ocean shear and stratification to estimate upper ocean boundary layer mixing rates. This approach implicitly parameterizes surface wave effects in terms of these inputs. Here we test this assumption using parallel experiments in a lake with small waves and in the open ocean with much bigger waves. Under the same wind stress and adjusting for buoyancy flux, we find the mixed layer average turbulent vertical kinetic energy in the open ocean typically twice that in the lake. The increase is consistent with models of Langmuir turbulence, in which the wave Stokes drift, and not wave breaking, is the dominant mechanism by which waves energize turbulence in the mixed layer. Applying these same theories globally, we find enhanced mixing and deeper mixed layers resulting from the inclusion of Langmuir turbulence in the boundary layer parameterization, especially in the Southern Ocean. **Citation:** D'Asaro, E. A., J. Thomson, A. Y. Shcherbina, R. R. Harcourt, M. F. Cronin, M. A. Hemer, and B. Fox-Kemper (2014), Quantifying upper ocean turbulence driven by surface waves, *Geophys. Res. Lett.*, *41*, 102–107, doi:10.1002/2013GL058193.

1. Introduction

[2] Turbulence in the upper boundary layer of the ocean mediates heat, momentum, and gas fluxes between the ocean and the atmosphere and is thus a key player in the climate system. The current generation of climate models typically have large errors of both signs in boundary layer thickness [*Belcher et al.*, 2012; *Fox-Kemper et al.*, 2011]. Since biological primary production is concentrated in this layer and its thickness strongly influences the available light, correct modeling of its thickness is critical for biogeochemical modeling. In particular, the models consistently underpredict boundary layer thickness in the Southern Ocean [*Sallee et al.*, 2013]. These Southern Ocean layers are major conduits for atmospheric heat, freshwater, and gasses, including CO_2, into the ocean interior. Significant errors in layer properties may indicate or cause significant errors in the rates at which these quantities are sequestered. Model errors in layer depth may reflect errors in air-sea forcing [*Bates et al.*, 2012], or errors in mixing parameterizations, which we discuss in this paper.

[3] Although surface wave processes appear explicitly in turbulence resolving models of the boundary layer [*Sullivan and McWilliams*, 2010] the current generation of climate models use parameterizations of upper ocean mixing that are forced by air-sea fluxes of momentum, heat, and salt with no explicit dependence on surface waves. The correlation between mixing rates and air-sea fluxes that supports these models may mask the role of surface waves in the mixing processes. This deficit partially results from the lack of comprehensive measurements of the properties of boundary layer turbulence [*D'Asaro*, 2014] and clear demonstrations of their dependence on surface waves. Here we provide such a demonstration.

[4] Two mechanisms most prominently link surface waves to boundary layer turbulence. Surface waves break, creating patches of turbulence [*Melville*, 1996], thereby playing a major role in controlling air-sea fluxes and increasing near-surface turbulent dissipation by several orders of magnitude [*Agrawal et al.*, 1992]. However, the wave-induced turbulence decays rapidly away from the surface, so that its effect on turbulence levels in the bulk of the mixed layer and at the mixed layer base is significantly less than at the surface. In a second less obvious effect, the Stokes drift [*Stokes*, 1847] of the waves (their nonlinear horizontal transport) rotates vertically aligned vortices into the downwave direction, leading to an instability of the wind-forced surface shear [*Craik and Leibovich*, 1976; *Leibovich*, 1983], henceforth CL. In its most idealized formulation, this mechanism creates steady counter-rotating vortices similar to the circulations first observed by Irving Langmuir [*Langmuir*, 1938] and commonly called "Langmuir circulations". More realistic predictions emerge from Large Eddy Simulations (LES) of the CL equations [*McWilliams et al.*, 1997; *Skyllingstad and Denbo*, 1995]. This simulated "Langmuir turbulence" includes transient Langmuir cells with patterns of surface convergence [*Thorpe*, 2004; *Zedel and Farmer*, 1991; *Smith*, 1998; *Pleuddemann et al.*, 1996] and downwelling [*Weller and Price*, 1988] similar to those observed [*Farmer and Li*, 1995; *Kukulka et al.*, 2009]. The LES predictions of bulk turbulence level can be summarized in a simple scaling [*Harcourt and D'Asaro*, 2008], which we test here.

Additional supporting information may be found in the online version of this article.

[1]Applied Physics Laboratory, University of Washington, Seattle, Washington, USA.
[2]School of Oceanography, University of Washington, Seattle, Washington, USA.
[3]Department of Civil and Environmental Engineering, University of Washington, Seattle, Washington, USA.
[4]Pacific Marine Environmental Laboratory, National Oceanic and Atmospheric Administration, Seattle, Washington, USA.
[5]Centre for Australian Weather and Climate Research, CSIRO Marine and Atmospheric Research, Hobart, Tasmania, Australia.
[6]Department of Geological Sciences, Brown University, Providence, Rhode Island, USA.

Corresponding author: E. A. D'Asaro, Applied Physics Laboratory, University of Washington, Seattle, WA 98105, USA. (dasaro@apl.washington.edu)

0094-8276/14/10.1002/2013GL058193

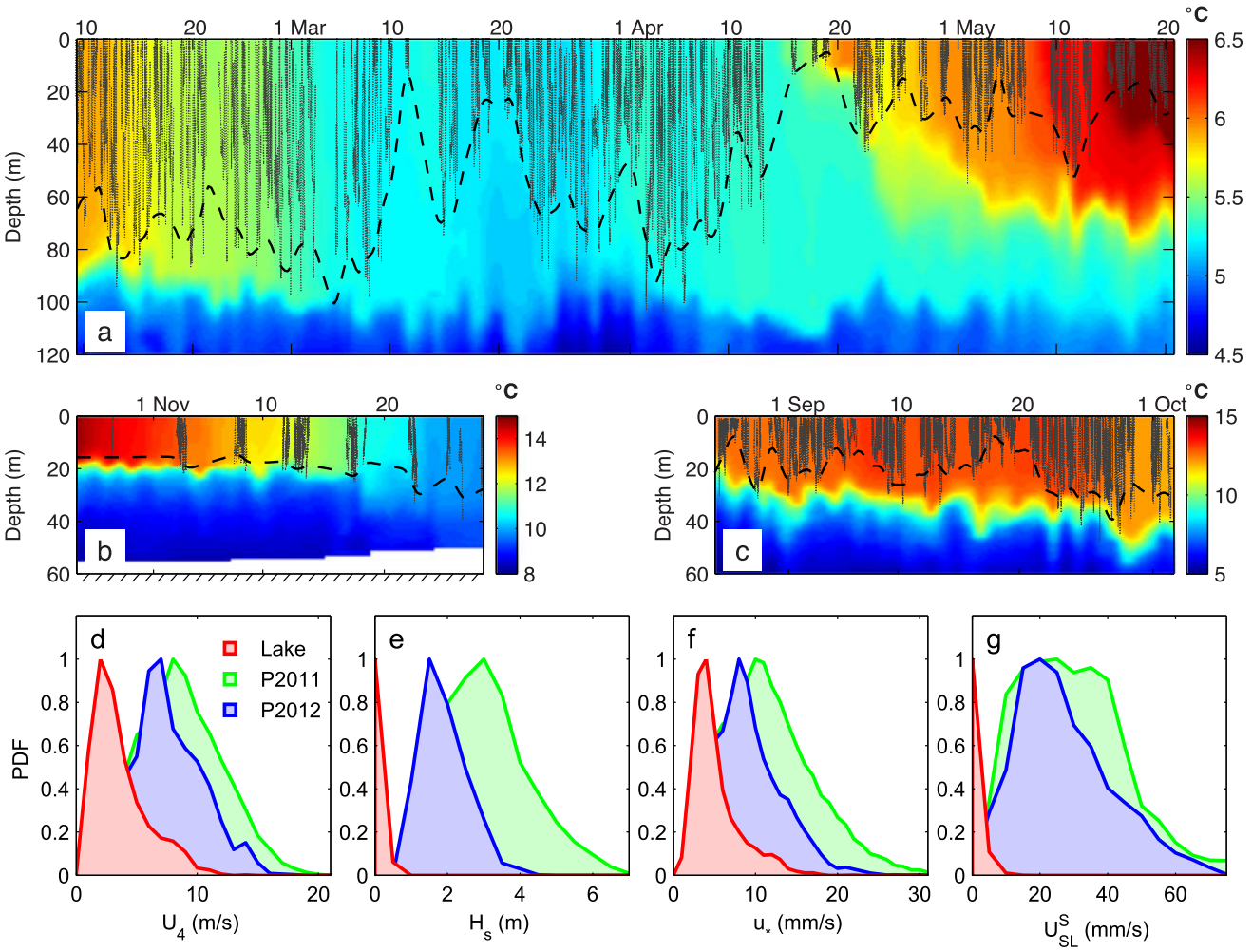

Figure 1. Ocean and atmospheric conditions during (a) open ocean measurements at Ocean Station P during winter 2011, (b) during summer/fall 2012, and (c) at Lake Washington during late fall 2011. Depth and time scales on all three panels are the same. Colors show temperature, dashed lines shows mixed layer depth, light dotted lines show float drift trajectories used in the analysis. Bottom row of figures compare histograms of (d) wind speed at 4 m, (e) significant wave height, (f) friction velocity, and (g) surface layer Stokes drift.

2. Observations

[5] Three parallel observation sets, using nearly identical equipment, were conducted with moderate wind forcing ($8-15\,\mathrm{m\,s^{-1}}$) but very different wave conditions. Typical open ocean conditions were measured at Ocean Station Papa (ocean weather station (OWS)-P 50°N, 145°W), a canonical site for upper ocean measurements [*Freeland*, 2007] due to its combination of strong wind forcing and weak mean and mesoscale eddy flows. Measurements for 100 days in the winter and spring of 2011 (Figure 1a) and another for 38 days in late summer of 2012 (Figure 1c) captured the deepest mixed layers (∼90 m) and shallowest mixed layers (∼20 m) of the year. A long-term surface buoy measured meteorological data necessary to compute air-sea fluxes. A Datawell Waverider measured directional surface wave spectra to compute the vertical profile of Stokes drift. Winds and waves were highest in winter, with typical values of $9\,\mathrm{m\,s^{-1}}$ and 3 m significant wave height (Figures 1d and 1e) and somewhat less in summer ($8\,\mathrm{m\,s^{-1}}$ and 2 m). Additional data plots and instrumental and data processing details are presented in the supporting information section 2 (section S2).

[6] Much smaller waves but similar winds were measured during eight storms in Lake Washington near Seattle, Washington (section S3) in the fall of 2011 (Figure 1b). The shoreline and two floating bridges (Figures S1a and S1b) limited wave fetch to less than 5 km. Mixed layer depths were nearly constant at 18–25 m (Figure 1b). Meteorological and wave measurements were made from a surface buoy and a Datawell Waverider. An acoustic anemometer measured stress using the dissipation method. Wind speeds during the measurements often reached $10\,\mathrm{m\,s^{-1}}$, as at OWS-P, but the waves never exceeded 0.5 m (Figure 1e). Winds varied little over the experimental region (section S3.6).

[7] The air-sea fluxes of heat Q and momentum $\tau = \rho u_*^2$ (ρ is water density, u_* is the friction velocity) are critical for evaluating our hypotheses. The fluxes at both sites were computed using the Coupled Ocean-Atmosphere Response Experiment (COARE) 3.0 formulae [*Fairall et al.*, 2003]; (sections S2.3 and S3.5). These parameterize the effects of surface waves and do not directly use surface wave data. At OWS-P, the errors introduced by this assumption were estimated from two COARE 3.0 variants that require wave measurements; these estimates of u_*

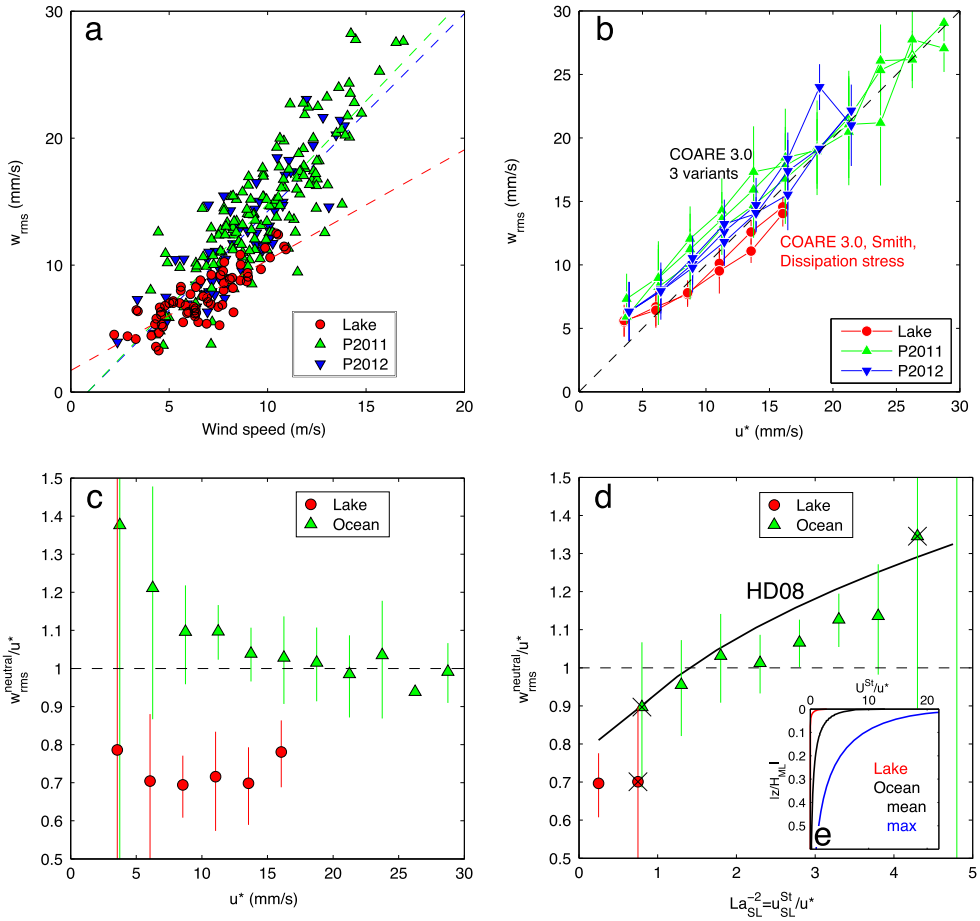

Figure 2. Mixed layer averaged turbulent vertical velocity w_{rms}. (a) w_{rms} from different deployments as a function of 4 m (measured) wind speed. Dashed lines are linear fits. (b) w_{rms} from different deployments as a function of u^*. For OWS-P, stress computed by three variants of the COARE 3.0 [*Fairall et al.*, 2003] surface roughness are shown (section S3.5); for the lake stress from COARE 3.0 with the Smith roughness [*Smith*, 1988] and from dissipation are shown (sections S2.2 and S2.3). (c) $w_{\mathrm{rms}}^{\mathrm{neutral}}/u_*$ averaged in bins of u_* for lake and ocean data. The COARE 3.0 with the Smith roughness is used. (d) $w_{\mathrm{rms}}^{\mathrm{neutral}}/u_*$ averaged in bins of inverse surface layer Langmuir number La_{SL} squared for lake and ocean data (see section 3). Heavy line is prediction of Langmuir turbulence [*Harcourt and D'Asaro*, 2008]. (e) Profiles of Stokes drift U^{St} averaged for lake (red), averaged for ocean (black) and the ocean profile with the maximum surface Stokes drift (blue). All confidence limits are 99%. Values of w_{rms} in Figures 2a and 2b are computed from the float pressure (section S4.2.1) with no additional corrections. Values of $w_{\mathrm{rms}}^{\mathrm{neutral}}$ in Figures 2c and 2d are corrected for finite float size and buoyancy flux (sections S4.2.3 and S4.2.4). In all panels, the lake (red) has a lower value of w_{rms} than does the ocean (green for 2011, blue for 2012) for the same atmospheric forcing.

averaged 6–10% lower (Figure S3). In Lake Washington, dissipation-based estimates of u_* (sections S3.1, S3.4, and S3.5) averaged 8% lower than COARE 3.0 during the measurement times. Computed heat fluxes matched the decrease in water column heat content to 12% (Figure S7). In Lake Washington 2–3% of the momentum fluxed out of the atmosphere by the wind stress propagated away in the surface wave field and was not available to drive the local boundary layer; this fraction was significantly less at OWS-P (section S3.7).

[8] The ocean's response to these air-sea fluxes and wave forcing was quantified by the average turbulent vertical kinetic energy within the mixed layer $0.5w_{\mathrm{rms}}^2$. This was measured using subsurface neutrally buoyant Lagrangian floats [*D'Asaro*, 2003] (section S4). During "Lagrangian drifts" (Figure S10) occupying most of each day, each float tracked the three-dimensional motion of water parcels, actively controlling its buoyancy to match that of the mixed layer and opening a horizontal drogue to increase its vertical drag [*D'Asaro et al.*, 1996; *Harcourt and D'Asaro*, 2010]. Float trajectories nearly uniformly fill the upper layer (Figure S10), so that the average along these trajectories is approximately the layer average. The vertical velocity w of the float was computed (section S4.2) from the change in measured pressure. We use w_{rms} the square root of the average of the squared vertical velocity to measure the mixed layer average turbulent intensity. The large vertical velocities due to surface waves are naturally filtered from these averages because pressure is constant along the Lagrangian trajectories of surface waves (section S4.2.1). Between Lagrangian drifts, at least daily, each float profiled vertically from beneath the mixed layer to the surface, thereby measuring the density stratification (Figures 1a–1c) and communicating by satellite with operators.

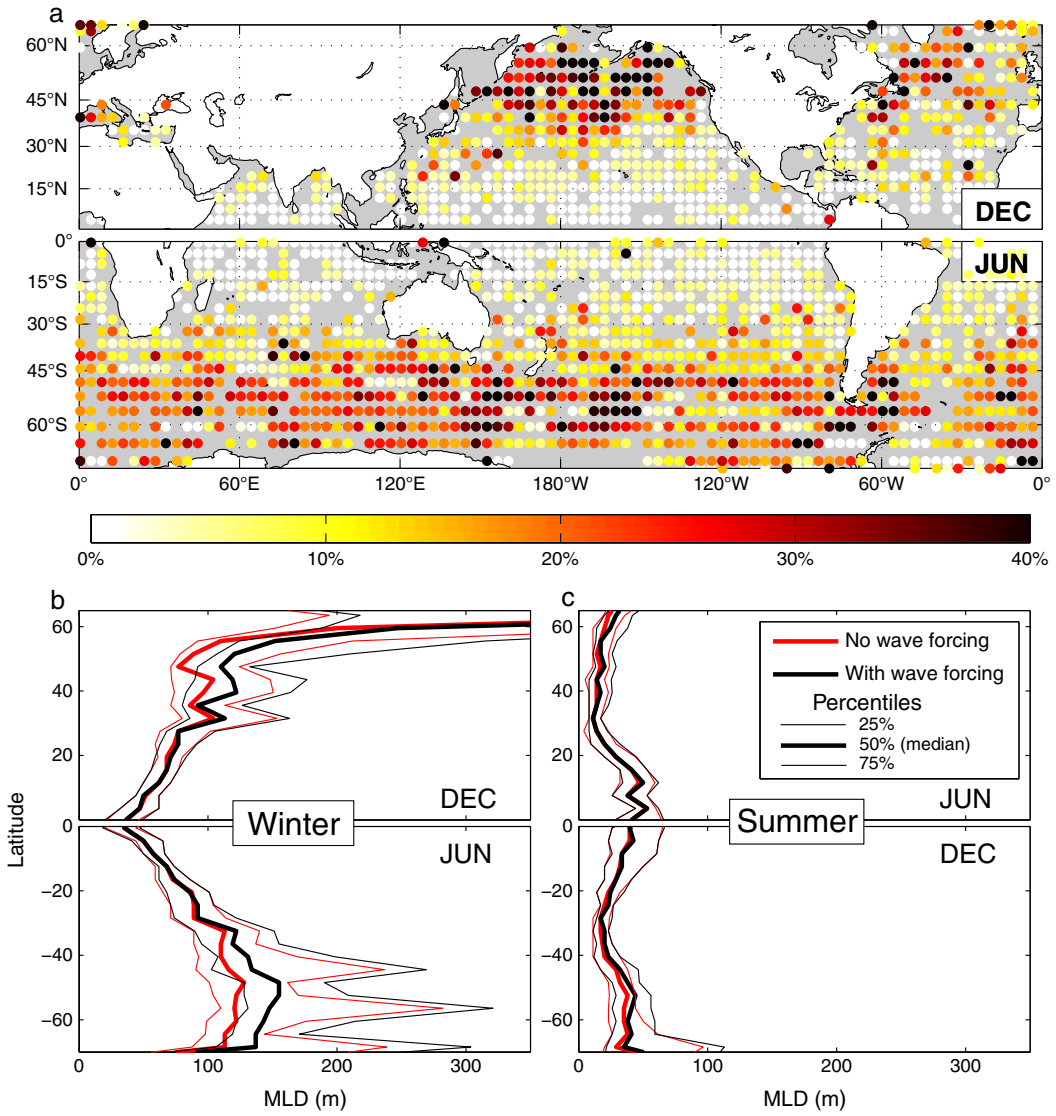

Figure 3. Contribution of Langmuir turbulence to global mixed layer depth. (a) Percentage increase in mixed layer depth with wave forcing relative to no wave forcing when Langmuir turbulence is parameterized [*Harcourt*, 2013] into a 1-D mixed layer model (section S7) 180 days after a near-summer solstice initial profile; (b) Zonal median (thick line) mixed layer depth and 25th and 75th percentiles (thin lines) 180 days after near-summer solstice initial profile Ð with (black) and without (red) wave forcing; (c) As for Figure 3b 365 days after initial profile.

[9] Buoyancy of the floats induces errors in the measurement of w_{rms} [*Harcourt and D'Asaro*, 2010]. The resulting vertical motion of the float relative to the water (section S4.2.2) changes both the measured vertical velocity and causes the mixed layer to be nonuniformly sampled. The floats' buoyancy was calibrated at least daily, with some low-wind days dedicated to calibration profiles. Direct measurements of float-relative velocity in Lake Washington imply buoyancy errors in w_{rms} of less than 5% (section S4.2.3). The finite size of the float also introduces errors by averaging smaller turbulent eddies. We correct for this by fitting a universal spectral form to the vertical velocity spectrum (section S4.2.5) for each drift and removing the component due to finite float size. This correction increases w_{rms} by 10–20% from the measured value and introduces uncertainties of 7% into the corrected w_{rms}.

[10] In summary, we measured the turbulent component of w_{rms} averaged across the mixed layer for winds of 8–15 m s^{-1}, mixed layer depths of 20–100 m and waves of 0.05–7 m. The wide range of wave conditions for the same wind speed allows us to assess whether waves are important and ask whether Langmuir turbulence can explain the measured effect.

3. Theory

[11] Models of Langmuir turbulence predict w_{rms} from u_*, the Stokes drift profile $\overline{u^S}(z)$, the mixed layer thickness H, and the air-sea buoyancy flux $B = g\alpha c_w^{-1} Q$, where g is the acceleration of gravity, α is the thermal expansion coefficient of seawater, and c_w^{-1} is its specific heat; we ignore small salinity effects. For monochromatic surface waves, $\overline{u^S}(z) = \overline{u^S}(0)e^{kz}$, where k is the horizontal wave number of the surface waves and z increases upward. Real surface waves have a broadband spectrum producing a profile $\overline{u^S}(z)$ that is the sum of many such decreasing exponentials. Waves with the

largest k cause $\overline{u^S}(z)$ to decrease rapidly away from the surface, but have little effect on the bulk energetics of the mixed layer. These effects are captured [*Harcourt and D'Asaro*, 2008] by the "surface layer Langmuir number" $La_{\mathrm{SL}} = (u_*/\overline{u^S_{\mathrm{SL}}})^{\frac{1}{2}}$, where $\overline{u^S_{\mathrm{SL}}} = (0.2H)^{-1}\int_{-0.2H}^{0}\overline{u^S}(z)\mathrm{d}z - u^S(z_{\mathrm{ref}})$, i.e., the average of the Stokes drift over the top 20% of the mixed layer, relative to the drift at a reference level $z_{\mathrm{ref}} = -0.75H$. For $B = 0$, steady forcing and purely wind-forced waves, LES studies [*Harcourt and D'Asaro*, 2008; *Van Roekel et al.*, 2012] find $w_{\mathrm{rms}}/u_* = \mathcal{F}(La_{\mathrm{SL}})$. This formulation parameterizes the dependence of w_{rms}/u_* on the ratio D_S/H, where D_S is an effective Stokes decay scale, i.e., $u^S(D_S)/u^S(0) = e^{-1}$. Both the surface Stokes drift and D_S/H are small in the lake compared to the ocean (Figure 2e); both contribute to the predicted smaller value of w_{rms}/u_*. This theory (black line, Figure 2d), predicts w_{rms}/u_* increasing from 0.8 with no waves to about 1 for typical ocean waves.

[12] Air-sea buoyancy flux can also force boundary layer turbulence. Surface cooling alone will drive a convective boundary layer with $w^2_{\mathrm{rms}} = aw^2_*$, where $w^3_* = BH$ and a is in the range [*Steffen and D'Asaro*, 2002] of 0.3–0.5. For the combined effect of B and La_{SL} additional simulations of Langmuir turbulence were conducted (section S5.1). They indicate that for a given La_{SL}, buoyancy flux increases w^2_{rms} by $(w^B_{\mathrm{rms}})^2 = 0.3w^2_* \; sign(w_*)$. We compensate for this by defining a "neutral" rms vertical velocity $(w^{\mathrm{neutral}}_{\mathrm{rms}})^2 = w^2_{\mathrm{rms}} - (w^B_{\mathrm{rms}})^2$ and modeling the combined effects of wind, waves, and buoyancy flux as $w^{\mathrm{neutral}}_{\mathrm{rms}}/u_* = \mathcal{F}(La_{\mathrm{SL}})$. Misalignment of the wind and waves (section S5.3) is a small effect.

4. Results

[13] The values of w_{rms} and $w^{\mathrm{neutral}}_{\mathrm{rms}}/u_*$ in Lake Washington (red) are less than those at OWS-P (green, blue) for the same wind forcing in all panels of Figure 2. The lake values are lower regardless of whether the effects of air-sea buoyancy flux and finite float size are included (i.e., Figures 2a and 2b versus Figures 2c and 2d); regardless of whether they are plotted against wind speed (Figure 2a), wind stress (Figures 2b and 2c), or Langmuir number (Figure 2d) or averaged in depth or time (Figure 2 versus Figure S13) or normalized by u_* (Figures 2c and 2d) or not (Figures 2a and 2b). For u_* between 8 and 16 mm s^{-1}, $w^{\mathrm{neutral}}_{\mathrm{rms}}/u_*$ averages 0.69 ± 0.03 for the lake and 1.05 ± 0.05 for OWS-P; the uncertainties are 95% confidence limits assuming a normal distribution and 1 degree of freedom for each drift segment. Possible instrumentation and parameterization biases (rms) from the finite float size, float buoyancy, correction to $w^{\mathrm{neutral}}_{\mathrm{rms}}$ and wave biases in u_* are 7%, 5%, 5%, and 8%, respectively. A formal error analysis based on these estimates (section S4.3) yields a 1.4% probability that the mean value of $w^{\mathrm{neutral}}_{\mathrm{rms}}/u_*$ in the lake is the same or greater than that at OWS-P.

[14] These observations are consistent with the predictions of Langmuir turbulence theory. The value of $w^{\mathrm{neutral}}_{\mathrm{rms}}/u_*$ increases with La_{SL} (Figure 2d) as predicted [*Harcourt and D'Asaro*, 2008] (black line) with an average level about 8% below the prediction. We conclude first that the scaled vertical kinetic energy in the mixed layer is weaker in Lake Washington than at OWS-P; second, that this difference is likely due to the much larger surface waves at OWS-P; and finally, that the Craik–Leibovich mechanism, e.g., Langmuir circulations, explains nearly all of this difference.

5. Discussion

[15] Based on these results there is no need to invoke wave forcing, by CL dynamics or otherwise, to explain the mixed layer averaged turbulent vertical kinetic energy where the waves are small, such as in lakes or estuaries; wind stress alone is sufficient. A small role for waves when they are small is intuitively sensible and consistent with other measurements [*Lien et al.*, 2008; *Gargett*, 2009]. Surface convergences, often thought to be characteristic of Langmuir circulations, can be formed in wind-forced simulations without the CL mechanism [*Skyllingstad and Denbo*, 1995; *Lien et al.*, 2008]. Our observations do not necessarily exclude wave breaking [*Craig and Banner*, 1994] or other proposed mechanisms [*Babanin*, 2006] for forcing boundary layer turbulence by waves or invalidate the crucial role played by surface waves in controlling the air-sea fluxes or in setting near-surface turbulent properties [*Terray et al.*, 1996]. Other measures of the boundary layer turbulence, particularly those focussing on near-surface properties, may not provide as good a match with Langmuir turbulence theory. Furthermore, none of these considerations invalidate the strong correlation between wind stress and turbulent intensity both in data, e.g., Figure 2b, and most theories of boundary layer turbulence, including Langmuir turbulence theory.

[16] Irving Langmuir's pioneering observations of Langmuir circulations in Lake George, made under conditions similar to our Lake Washington measurements (section S6), were inspired by his observations of long lines of floating seaweed in the Atlantic ocean, made under conditions similar to our OWS-P measurements. Our results suggest that the CL mechanism only played a significant role in Langmuir's open ocean observations; in Lake George, the circulations he observed may well have been driven primarily by wind stress.

6. Implications

[17] Returning to the issues raised in section 1, we test the global implications of our results by simulating (section S7) the annual cycle of the boundary layer with a 1-D, depth-time model of boundary layer mixing driven by Langmuir turbulence [*Harcourt*, 2013] and tuned to be consistent with the LES predictions [*Harcourt and D'Asaro*, 2008] of entrainment rate. A set of depth-time calculations initialized by measured ARGO float profiles were driven by a typical year of atmospheric forcing (Figure 3). Identical calculations with and without CL wave forcing, show waves to have little effect at tropical or subtropical latitudes, but to increase simulated boundary layer depths at high latitudes by 15–20% on average. This supports arguments [*Belcher et al.*, 2012] that the effects of waves in enhancing boundary layer turbulence varies geographically and may explain some climate model biases in mixed layer depth. The contribution of surface wave generated turbulence within these models is unlikely to be properly included without consideration of the geographical variations in surface waves. In a changing climate, the distributions of both wind and waves, and perhaps their relative importance in driving mixing, is likely to change [*Hemer et al.*, 2013].

[18] **Acknowledgments.** E.A.D., J.T., R.R.H., and A.S. were supported by National Science Foundation grants OCE0850551 and OCE0934580. The technical staff of APL-UW were essential to making these measurements. The 53rd Air Force Reserve, Weather Reconnaissance

Squadron air-deployed the first float at OWS-P; the CCGS *John P. Tully* recovered it and deployed the second float which the R/V *New Horizon* recovered. Support for the OWS-P meteorological mooring is provided by NOAA Climate Observation Program. The Argo data were collected and made available freely by the International Argo Program and the national programs that contribute to it. The Argo Program is part of the Global Ocean Observing System. B.F.K. was supported by NSF 0934737, 1258907, and NASA NNX09AF38G.

[19] The Editor thanks two anonymous reviewers for assistance evaluating this manuscript.

References

Agrawal, Y., E. Terray, M. Donelan, P. Hwang, A. Williams III, W. Drennan, K. Kahma, and S. Kitaigorodskii (1992), Enhanced dissipation of kinetic energy beneath surface waves, *Nature*, *359*(6392), 219–220.

Babanin, A. V. (2006), On a wave-induced turbulence and a wave-mixed upper ocean layer, *Geophys. Res. Lett.*, *33*, L20605, doi:10.1029/2006GL027308.

Bates, S. C., B. Fox-Kemper, S. R. Jayne, W. G. Large, S. Stevenson, and S. G. Yeager (2012), Mean biases, variability, and trends in air-sea fluxes and SST in the CCSM4, *J. Clim.*, *25*(22), 7781–7801.

Belcher, S. E., et al. (2012), A global perspective on Langmuir turbulence in the ocean surface boundary layer, *Geophys. Res. Lett.*, *39*, L18605, doi:10.1029/2012GL052932.

Craig, P., and M. L. Banner (1994), Modeling wave-enhanced turbulence in the ocean surface layer, *J. Phys. Oceanogr.*, *24*, 2546–2559.

Craik, A. D. D., and S. Leibovich (1976), A rational model for Langmuir circulations, *J. Fluid Mech.*, *73*, 401–426, doi:10.1017/S0022112076001420.

D'Asaro, E. A. (2003), Performance of autonomous Lagrangian floats, *J. Atmos. Oceanic Technol.*, *20*(6), 896–911.

D'Asaro, E. A. (2014), Turbulence in the upper-ocean mixed layer, *Annu. Rev. Mar. Sci.*, *6*(6), doi:10.1146/annurev-marine-010213-135138.

D'Asaro, E. A., D. M. Farmer, J. T. Osse, and G. T. Dairiki (1996), A Lagrangian float, *J. Atmos. Oceanic Technol.*, *13*(6), 1230–1246.

Fairall, C., E. F. Bradley, J. E. Hare, A. A. Grachev, and J. B. Edson (2003), Bulk parameterization of air–sea fluxes: Updates and verification for the COARE algorithm, *J. Clim.*, *16*, 571–591, doi:10.1175/1520-0442(2003)016<0571:BPOASF>2.0.CO;2.

Farmer, D. M., and M. Li (1995), Patterns of bubble clouds organized by Langmuir circulation, *J. Phys. Oceanogr.*, *25*(6), 1426–1440.

Fox-Kemper, B., G. Danabasoglu, R. Ferrari, S. M. Griffies, R. W. Hallberg, M. M. Holland, M. E. Maltrud, S. Peacock, and B. L. Samuels (2011), Parameterization of mixed layer eddies. III: Implementation and impact in global ocean climate simulations, *Ocean Modell.*, *39*, 61–78.

Freeland, H. (2007), A short history of ocean station Papa and Line P, *Prog. Oceanogr.*, *75*(2), 120–125, doi:10.1016/j.pocean.2007.08.005.

Gargett, A. E. (2009), Couette vs. Langmuir circulations: Comment on "On the helical flow of Langmuir circulation — Approaching the process of suspension freezing" by Dethleff, Kempema, Koch and Chubarenko, *Cold Reg. Sci. Technol.*, *56* (1), 58–60, doi:10.1016/j.coldregions.2008.10.003.

Harcourt, R. R. (2013), A second moment closure model of Langmuir turbulence, *J. Phys. Oceanogr.*, *43*, 673–697, doi:10.1175/JPO-D-12-0105.1.

Harcourt, R. R., and E. A. D'Asaro (2008), Large eddy simulation of Langmuir turbulence in pure wind seas, *J. Phys. Oceanogr.*, *38*, 1542–1562, doi:10.1175/2007JPO3842.1.

Harcourt, R. R., and E. A. D'Asaro (2010), Measurement of vertical kinetic energy and vertical velocity skewness in oceanic boundary layers by imperfectly Lagrangian floats, *J. Atmos. Oceanic Technol.*, *27*, 1918–1935, doi:10.1175/2010JTECHO731.1.

Hemer, M., Y. Fan, N. Mori, A. Semedo, and X. Wang (2013), Projected future changes in wind-wave climate in a multi-model ensemble, *Nat. Clim. Change*, *3*(5), 471–476.

Kukulka, T., A. J. Plueddemann, J. H. Trowbridge, and P. P. Sullivan (2009), Significance of Langmuir circulation in upper ocean mixing: Comparison of observations and simulations, *Geophys. Res. Lett.*, *36*, L10603, doi:10.1029/2009GL037620.

Langmuir, I. (1938), Surface motion of water induced by wind, *Science*, *87*, 119–123.

Leibovich, S. (1983), The form and dynamics of Langmuir circulations, *Annu. Rev. Fluid Mech.*, *15*, 391–427.

McWilliams, J., P. Sullivan, and C. Moeng (1997), Langmuir turbulence in the ocean, *J. Fluid Mech.*, *334*, 1–30.

Melville, W. K. (1996), The role of surface-wave breaking in air-sea interaction, *Annu. Rev. Fluid Mech.*, *28*, 279–321.

Pleuddemann, A., J. Smith, D. Farmer, R. Weller, W. Crawford, R. Pinkel, S. Vagle, and A. Gnanadesikan (1996), Structure and variability of Langmuir circulations during the surface waves processes program, *J. Geophys. Res.*, *101*, 3525–3543.

Lien, R.-C., T. B. Sanford, and W.-T. Tsai (2008), Observations of turbulence mixing and vorticity in a littoral surface boundary layer, *J. Phys. Oceanogr.*, *38*, 648–669, doi:10.1175/2007JPO3469.1.

Sallée, J.-B., E. Shuckburgh, N. Bruneau, A. J. S. Meijers, T. J. Bracegirdle, and Z. Wang (2013), Assessment of Southern Ocean mixed-layer depths in CMIP5 models: Historical bias and forcing response, *J. Geophys. Res. Oceans*, *118*, 1845–1862, doi:10.1002/jgrc.20157.

Skyllingstad, E., and D. Denbo (1995), An ocean large-eddy simulation of Langmuir circulations and convection in the surface mixed layer, *J. Geophys. Res.*, *100*, 8501–8522.

Smith, J. (1998), Evolution of Langmuir circulation during a storm, *J. Geophys. Res.*, *103*(C6), 12,649–12,668.

Smith, S. D. (1988), Coefficients for sea surface wind stress, heat flux, and wind profiles as a function of wind speed and temperature, *J. Geophys. Res.*, *93*(C12), 15,467–15,472.

Steffen, E., and E. D'Asaro (2002), Deep convection in the Labrador Sea as observed by Lagrangian floats, *J. Phys. Oceanogr.*, *32*(2), 475–492.

Stokes, G. G. (1847), On the theory of oscillatory waves, *Trans. Cambridge Philos. Soc.*, *8*, 441–455.

Sullivan, P., and J. McWilliams (2010), Dynamics of winds and currents coupled to surface waves, *Annu. Rev. Fluid Mech.*, *42*, 19–42.

Terray, E. A., M. A. Donelan, Y. C. Agrawal, W. M. Drennan, K. K. Kahma, A. J. Williams III, P. A. Hwang, and S. A. Kitaigorodskii (1996), Estimates of kinetic energy dissipation under breaking waves, *J. Phys. Oceanogr.*, *26*(5), 792–807.

Thorpe, S. (2004), Langmuir circulation, *Annu. Rev. Fluid Mech.*, *36*, 55–79, doi:10.1146/annurev.fluid.36.052203.071431.

Van Roekel, L. P., B. Fox-Kemper, P. P. Sullivan, P. E. Hamlington, and S. R. Haney (2012), The form and orientation of Langmuir cells for misaligned winds and waves, *J. Geophys. Res.*, *117*, C05001, doi:10.1029/2011JC007516.

Weller, R., and J. F. Price (1988), Langmuir circulation within the oceanic mixed layer, *Deep Sea Res.*, *35*, 711–747.

Zedel, L., and D. M. Farmer (1991), Organized structures in subsurface bubble clouds: Langmuir circulation in the open ocean, *J. Geophys. Res.*, *96*(C5), 8889–8900, doi:10.1029/91JC00189.